Journal of Statistical Physics, Vol. 27, No. 1, 1982

Percolation Analysis of Stochastic Models of Galactic Evolution

Lawrence S. Schulman[1] and Philip E. Seiden[2]

Received February 12, 1981

The stochastic star formation model of galactic evolution can be cast as a problem of directed percolation, the time dimension being that along which the directed bonds exist. We study various aspects of this percolation, those of general interest for the percolation phase transition and those of particular importance for the astrophysical application. Both analytical calculations and computer simulations are provided and the results compared. Among the properties are: value of the percolation threshold, critical indices, percolation probability (star density) near and away from the critical point, local density, cluster sizes, effects of rotation (for disk galaxy models) on the percolation threshold. Astrophysical consequences of some of these properties are discussed, in particular the way in which general phase transition behavior contributes to spiral arm morphology. We look at 1 (space) + 1 (time), 2 + 1 and "∞" + 1 dimensions, the 2 + 1 case being of interest for disk galaxies.

KEY WORDS: Star formation-stochastic; percolation-directed; galactic evolution; stochastic process.

1. INTRODUCTION

The phenomenon of percolation has applications in diverse areas and has been extensively investigated over the last decade. However, the class of percolation problems where one or more dimensions is directed has received little attention. In this paper we describe a class of problems having one directed dimension, and will investigate, in particular, the cases of 1 + 1, 2 + 1, and "∞" + 1 dimensions. The first number refers to the nondirected dimensions and the 1 following the plus sign refers to the single directed dimension.

[1] IBM Thomas J. Watson Research Center, Yorktown Heights, New York 10598 and Physics Department, Technion, Haifa, Israel.

[2] IBM Thomas J. Watson Research Center, Yorktown Heights, New York 10598.

0022-4715/82/0100-0083$03.00/0

The impetus for considering this class of problems comes from an active area of astrophysics concerning the structure and evolution of galaxies. In a series of recent papers,[1–4] it has been proposed that the main factor determining galactic evolution is the star-forming process and that the process that creates the major fraction of stars is stochastic self-propagating star formation. In this mechanism stars are created under the direct influence of other stars. Massive stars (masses $\gtrsim 5$ solar masses) have short and violent life cycles. They will completely evolve in periods of the order of ten million years and end their lives as supernovas. By means of the shock wave created by the supernova (or even by the high-energy densities radiated during the star's lifetime) the interstellar gas can be compressed to densities high enough to allow gravity to finish the collapse into stars. If at least one of these new stars is a high-mass star the process can repeat itself, leading to the conversion of the primordial galactic gas into aggregates of stars.

This process is equivalent to a percolation problem in which star formation percolates in both space and time. The existence of a bright, massive star at any given time is connected to that of stars at earlier or later times only. Time is the directed dimension in the problem.

The main emphasis in the galactic problem has been on disk galaxies (e.g., spirals), since it is in these galaxies that active star formation is presently occurring. Groups of stars created by this process (open clusters and associations) are of the order of 50–200 pc (parsecs) in size, the same order as the thickness of disk galaxies (1 pc $\simeq$ 3.3 light years). Therefore, for the purposes of the stochastic self-propagating star formation mechanism the spatial structure of the disk is two dimensional. For this reason primary interest is in the $(2+1)$-dimensional system, although we will also discuss the simpler $1+1$ and "∞"$+1$ systems.

This paper will concentrate on the properties of the underlying directed percolation process itself and we refer the reader elsewhere for the astronomical details[1–4] and for alternate theories of spiral arm formation.[5] The emphasis is on the determination of the critical parameters of the directed percolation problem. We present both analytical results and computer simulations and find that the agreement between them is generally quite good. We also compare our results to earlier work on directed percolation. In Section 2 we describe the lattice models that we use. In Sections 3, 4, and 5 we discuss "∞"$+1$, $1+1$, and $2+1$ dimensions, respectively. In Section 6, we summarize our results and conclusions.

2. LATTICE MODEL

To each point $\alpha = (i_1, i_2, \ldots, i_n)$ on an n-dimensional lattice assign a variable σ_α taking values 0 and 1. The system state, described by the set of

values of σ_α, evolves stochastically in time in the following way: For each α define a set R_α, the set of neighbors of α, whose definition in each case depends on lattice shape and dimension. Each neighbor β of α for which $\sigma_\beta = 1$ at time t has probability p of causing σ_α on the following generation (time $t + 1$) to take the value 1. Formally,

$$\sigma_\alpha(t+1) = 1 - \prod_{\beta \in R_\alpha} \left[1 - A_{\alpha,\beta,t}\sigma_\beta(t)\right]$$

where $A_{\alpha,\beta,t}$ is, for each α, β, and t, an independent random variable taking the value 1 with probability p and 0 with probability $1 - p$. The quantity $A_{\alpha,\beta,t}$ will at times be written $A(\alpha, \beta, t)$ or $A_{\alpha\beta t}$.

The significance of σ_α is that when it takes the value 1, there is a star (or more realistically a cluster of newly formed stars) in the cell (or at the site) α. Under this circumstance we shall sometimes refer to the site α as being "alive." The value 1 for the variable $A_{\alpha\beta t}$ represents the event that if there is a star at β at time t, then there will be one at α at $t + 1$.

Let $\rho(t)$ be the average of $\sigma_\alpha(t)$ over the lattice (at fixed t). For sufficiently small p $\rho = \lim_{t\to\infty} \rho(t)$ is 0 for any initial conditions. Above a certain critical value p_c this limit can be finite. Of interest is the value of p_c, the length distribution of (finite) clusters for $p < p_c$, the dependence of ρ on p for $p > p_c$, and the temporal length distribution of (necessarily finite) clusters for all $p < 1$ in the case of a finite lattice.

When the random variable $A_{\alpha,\beta,t}$ is 1 the sites α and β are said to be connected between times t and $t + 1$. Dense infinite clusters will exist if and only if there are sites α, for some arbitrary t, such that if $\sigma_\alpha(t)$ is 1, then $\rho(t) \to \rho > 0$. Hence p_c defined above is the percolation threshold. The asymptotic value of ρ for the initial condition $\sigma_\alpha(0) = 1$, all α, is the percolation probability, the probability that a site is part of an infinite cluster.

The systems of interest are as follows.

A. *Infinity-plus-one dimensions.* This is analogous to mean field theory in that all sites are connected to all other sites with an average probability $p = x/N$ where N is the number of sites. Hence R_α is the entire "lattice" (at a single t). Percolation is still directed since sites only connect to other sites at a later time.

B. *One-plus-one-dimensional percolation.* α (site label) runs over a one-dimensional lattice of N sites with periodic boundary conditions (and critical values are defined for $N \to \infty$). Calling the site label j (instead of α), $j = 1, \ldots, N$ and the set R_j is just $\{j - 1, j + 1\}$ (modulo N).

C. *Two-plus-one-dimensional percolation.* In the stochastic galactic evolution model the galaxy is represented as a series of N concentric annuli, each divided into $6N$ cells, each cell being approximately square (and about 600 light years on a side). A cell in this model usually has six

contiguous neighbors so that the geometry of the array is essentially that of a triangular lattice. An important feature of disk galaxies is their roughly axially symmetric rotation, a rotation that is not rigid so that the galaxy experiences an appreciable amount of shear. This shear will cause the aggregates of stars created by stochastic star formation to be spread out into the characteristic spiral arms of large disk galaxies.

In our analysis of the percolation process we consider only the two-dimensional triangular lattice; $\alpha = (i, j)$, $i, j = 1, \ldots, N$, with periodic boundary conditions. The shear is introduced by sliding the rows of the lattice with respect to each other so as to simulate the shear produced by the nonuniform galactic rotation. In the computer models we use an equivalent rectangular lattice where the neighbors are defined as those cells having contiguous boundaries with the cell of interest. Neglecting those rare occurrences where the cell boundaries exactly line up, the number of neighbors in this lattice is six, as in the triangular lattice.

With no shear the neighbors of α are the six nearest neighbors on the triangular lattice. With shear it is easiest to picture the sets R_α changing due to an active transformation on the lattice: rows i, $i_0 \leqslant i \leqslant N$ all move to the right and the neighbors at subsequent times are the nearest neighbors in the new configuration. Several neighbor shifts can occur in one time step. As we will see in Section 5, the shear affects the values of the critical parameters.

D. *Three-plus-one dimensions.* The case of three-plus-one dimensions is also of interest since it should be applicable to the case of elliptical galaxies.[4] We have, however, done only the most preliminary examination of this case and will not discuss it further in this paper.

3. INFINITY-PLUS-ONE-DIMENSIONAL PERCOLATION

We shall first do the mean field case as it is solvable and illustrates some of the techniques used in the other situations (similar models have been considered in population genetics[6]).

The evolution law is

$$\sigma_i(t+1) = 1 - \prod_{j=1}^{N} \left[1 - A_{ijt}\sigma_j(t)\right] \tag{1}$$

Suppose at time t exactly n of the variables $\sigma_i(t)$ take the value 1. Then $\rho(t) = n/N$ and

$$\sigma_i(t+1) = 1 - \prod_{j=1}^{n} (1 - A_{ijt}) \tag{2}$$

The expectation of $\rho(t+1)$ is therefore

$$\langle \rho(t+1) \rangle = 1 - (1-p)^n = 1 - \left(1 - \frac{x}{N}\right)^{N\rho(t)} \tag{3}$$

For large N this is (dropping the expectation symbol)

$$\rho(t+1) = 1 - e^{-x\rho(t)} \tag{4}$$

An equilibrium value of ρ must satisfy

$$\rho = 1 - e^{-x\rho} \tag{5}$$

$\rho = 0$ is always a solution, while for $x > 1$ there is a second solution so that the critical value is $x_c = 1$. Moreover, for $0 < x - x_c \ll 1$

$$\rho \sim \frac{2(x-1)}{x^2} \tag{6}$$

so that letting the critical exponent β be defined by

$$\rho = \text{const}(p - p_c)^{\beta} \tag{7}$$

we have $\beta = 1$ in this case. Equation (4) also gives the decay and equilibration properties for the expectation of $\rho(t)$.

Next we use a scaling argument to give x_c and to get the critical exponent associated with time correlations (cluster durations). We shall use single time step decimation. As defined above $A(i,j,t)$ is 1 if site i is connected to site j between time steps t and $t+1$ and 0 otherwise. Let $B(i,j,t)$ be the random variable for two-step connection: $B(i,j,t)$ is 1 if there is a path (i.e., with any intermediate site) from i at time t to j at time $t+2$. Clearly,

$$1 - B(i,j,t) = \prod_{k=1}^{N} \left[1 - A(i,k,t)A(k,j,t+1)\right] \tag{8}$$

Let the expectation of B be p', which is therefore the probability that a specific site at time t is connected to a specific site at $t+2$. Taking the expectation of (8) yields

$$1 - p' = (1 - p^2)^N \tag{9}$$

or with $p' = x'/N$ [neglecting $O(1/N^2)$ terms]

$$x' = x^2 \tag{10}$$

The new process, taking time steps of length 2 with probability x'/N, is exactly the same as the former aside from the change in probability. No correlations in connectivity have been introduced. Rescaling n times gives (with obvious notation)

$$x^{(n)} = x^{2n} \tag{11}$$

The fixed points are $x = 0$, 1, and ∞ an attractor, a repeller, and an attractor, respectively. Zero is the disconnected lattice, ∞ is the connected system. Equation (11) also gives the critical exponent ν for the time correlation length. If any characteristic length can be associated with the system, for example, for $x < x_c = 1$ the average cluster size, then successive transformations cut this length in half. Suppose

$$\xi(x) = k(x_c - x)^{-\nu} \tag{12}$$

describes the correlation length for $x < x_c$ (for some constant k). Then under a single scale transformation

$$k(x_c - x')^{-\nu} = \xi(x') = \tfrac{1}{2}\xi(x) = \tfrac{1}{2}k(x_c - x)^{-\nu} \tag{13}$$

For x near x_c, $x_c - x' \sim (\partial x'/\partial x)(x_c - x) = 2(x_c - x)$ and it follows from (13) that $\nu = 1$. Clearly what has been proved for ξ holds for any characteristic time scale in the system, for example, the length of clusters for $x > x_c$ which are not part of infinite clusters.

The conclusions for ξ for $x < 1$ can be verified explicitly by a nonscaling argument. First we give a particular definition of $\xi(x)$:

$$\xi = \sum_{t=0}^{\infty} tP_x(t) \tag{14}$$

where $P_x(t)$ is the probability of having a cluster of length t exactly.

To calculate $P_x(t)$, define $a(n,t)$ to be the probability that exactly n sites are alive at time t [so that $a(n,0) = \delta_{n0}$]. Since all sites are identical the system evolution is described by a transition matrix $W(k,j)$, the probability of going from j living sites to k living sites. Because we are interested in fixed j,k for $N \to \infty$ we can neglect the possibility that connections from two living sites at t hit the same site at $t+1$ (for $x > x_c$ there will be finite density and this effect is important). The probability of the given j live sites reaching a particular set of k sites is

$$\left(\frac{jx}{N}\right)^k \left(1 - \frac{jx}{N}\right)^{N-k}$$

The number of subsets of size k is $\binom{N}{k}$. Hence

$$W(k,j) = \binom{N}{k}\left(\frac{jx}{N}\right)^k \left(1 - \frac{jx}{N}\right)^{N-k} = \frac{(jx)^k e^{-jx}}{k!}, \qquad j,k \geqslant 0 \tag{15}$$

the second equality being the limiting form for $N \to \infty$. The coefficients $a(n,t)$ satisfy

$$a(k,t+1) = \sum_j W(k,j)a(j,t)$$

The quantity $P_x(t)$ is given by

$$P_x(t) = \sum_{j>0} W(0,j)a(j,t) \tag{16}$$

The obvious fact that the average number of living sites should decrease by a factor of x on each time step is immediately verified

$$\langle k\rangle_{t+1} \equiv \sum_{k=0}^{\infty} ka(k,t+1) = \sum_{j,k=0}^{\infty} \frac{k(jx)^k e^{-jx}}{k!} a(j,t)$$

$$= x \sum_{j=0}^{\infty} ja(j,t) = x\langle k\rangle_t \tag{17}$$

For x close to 1, ξ becomes large and the growth of ξ might be expected to depend on only the largest eigenvalue of W. In fact, however, it depends on the largest eigenvalue of a truncation of W, for the following reason: W is a stochastic matrix; it has largest eigenvalue 1 with the obvious eigenvector $a(n) = \delta_{n0}$, since $n = 0$ is an absorbing state. The truncated matrix $W(k, j)$ for k and j both (strictly) greater than 0 is not stochastic and it is its largest eigenvalue that fixes the lifetime for staying away from the 0 state (for a similar calculation see Newman and Schulman[7]). Designate the truncation of W by W'. Let its largest eigenvalue be λ and the associated eigenvector u. Since all elements of W' are positive λ is real positive and u unique (Frobenius theorem). The demonstration (17) was true for all vectors and in particular for u. Hence

$$\langle n\rangle_{t+1} = x\langle n\rangle_t = x\sum ju_j \tag{18}$$

On the other hand,

$$\langle n\rangle_{t+1} = \sum jW'_{jk}u_k = \lambda \sum ju_j \tag{19}$$

Comparing, we have $\lambda = x$. As $x \to 1$ the large t behavior of $a(n,t)$ determines ξ and successive application of W to $a(n,0)$ causes all but the eigenvector associated with $\lambda = x$ to drop out. Consequently,

$$P_x(t) = \sum_{j>0} W(0,j)a(j,t) \sim \sum e^{-jx}\lambda^t u_j = x^t \sum u_j e^{-jx}$$

But we can also sum the identity

$$xu_k = \sum_{j=1}^{\infty} \frac{(jx)^k}{k!} e^{-jx} u_j$$

over k to get

$$\sum_{j=1}^{\infty} u_j e^{-jx} = 1 - x$$

It follows that

$$\xi(t) = \sum tP_x(t) \sim \sum tx^t(1-x) = \frac{1}{1-x} \tag{20}$$

and the critical exponent is explicitly seen to be 1.

4. ONE-PLUS-ONE-DIMENSIONAL PERCOLATION

The dynamical equation is

$$\sigma_i(t+1) = 1 - \prod_{j=i\pm 1} \left[1 - A_{ijt}\sigma_j(t)\right] \tag{21}$$

where $i \pm 1$ is understood to mean modulo N, with N the total number of sites. The simplest mean field theory of the evolution law (21) is gotten by taking expectation values and ignoring correlations. Writing $\rho(t) = \langle \sigma_i(t) \rangle$ for any i, we have

$$\rho(t+1) = 1 - \left[1 - p\rho(t)\right]^2 \tag{22}$$

where the expectation of all the A variables is p. The equilibrium equation is $[\rho(t) \equiv \rho]$

$$\rho\left[(p - \tfrac{1}{2}) - \tfrac{1}{2}p^2\rho\right] = 0 \tag{23}$$

Thus $\rho = 0$ is always a solution and for $p > \frac{1}{2}$ there is a positive solution ρ. Hence $p_c = \frac{1}{2}$ and β [cf. Eq. (7)] is 1.

We can improve on Eq. (22) by using a cumulant expansion.[8] The expectation of Eq. (21) is now written

$$\rho(t+1) = 1 - \left[1 - p\rho(t)\right]^2 - \left\langle \left[1 - p\sigma_{i+1}(t)\right]\left[1 - p\sigma_{i-1}(t)\right]\right\rangle_c \tag{24}$$

with

$$\langle UV \rangle_c = \langle UV \rangle - \langle U \rangle \langle V \rangle$$

for random variables U and V. Equation (24) simplifies to

$$\rho(t+1) = 2p\rho(t) - p^2\rho(t)^2 - p^2\langle \sigma_{i+1}(t)\sigma_{i-1}(t)\rangle_c \tag{25}$$

The cumulant in (25) can be expressed in terms of expectation values and higher order cumulants at time $t-1$. We cut off this potentially infinite regression in the calculation of $\langle \sigma_{i+1}(t)\sigma_{i-1}(t)\rangle_c$ by ignoring all second- or higher-order cumulants at time $t-1$. Thus

$$\begin{aligned}
&\langle \sigma_{i+1}(t)\sigma_{i-1}(t)\rangle_c \\
&\quad = \left\langle \left[p\sigma_i(t-1) + p\sigma_{i+2}(t-1) - p^2\sigma_i(t-1)\sigma_{i+2}(t-1)\right] \right. \\
&\qquad \left. \times \left[p\sigma_{i-2}(t-1) + p\sigma_i(t-1) - p^2\sigma_{i-2}(t-1)\sigma_i(t-1)\right]\right\rangle_c \\
&\quad = \bar{\rho}(1-\bar{\rho})p^2(1-p\bar{\rho})^2
\end{aligned} \tag{26}$$

with $\bar{\rho} = \rho(t-1)$. The cumulant in (26) is nonzero because terms σ_i^2 $(= \sigma_i)$ appear in the product. In equilibrium $\rho(t) \equiv \rho$ so that (26) and (25) combined yield

$$(1-\rho)(1-p\rho)^2 = (2p-1)/p^4 \tag{27}$$

where the solution $\rho = 0$ has been factored out. Equation (27) will begin to have a nonnegative solution for ρ when

$$p^4 - 2p + 1 = 0 \tag{28}$$

so that

$$p_c \cong 0.5437 \tag{29}$$

the root of (28). It is also clear that we still have $\beta = 1$.

The critical exponent ν [cf. Eq. (12)] can also be gotten quite simply. Go back to Eq. (22) and assume p is slightly below $p_c(= 1/2)$ and that

$$\rho(t) \sim \rho(t_0) e^{-(t-t_0)/\xi}$$

It follows that

$$\xi \sim \frac{1}{2(p_c - p)} \tag{30}$$

so that $\nu = 1$. This conclusion is unchanged when second-order cumulants are included.

Scale Transformation

We next use renormalization group methods for the critical behavior of this percolation problem. Specifically, we shall rescale time by a factor of 2 by "decimating" a single time step. With reference to Fig. 1, we want the probability that there is a connected path from A to F given that there is probability p for any of the (possible) connections A–B, A–D, C–F. The question as just phrased is in fact too restrictive. More extensive possibilities for bonds are considered and we begin by assuming that not only is

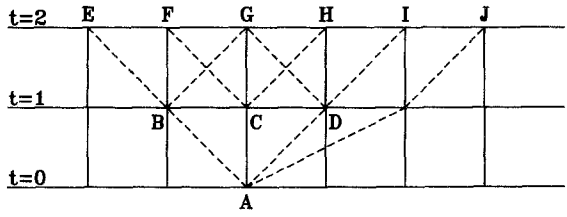

Fig. 1. Scale transformation by time step decimation. Labels A, B, etc. distinguish both position and time.

$\langle A(i, i \pm 1, t)\rangle$ nonzero (and equal to p) but also $\langle A(i,i,t)\rangle \equiv q$ and $\langle A(i, i \pm 2, t)\rangle \equiv r$ need not be zero. In Fig. 1 this implies, for example, that A and C are connected with probability q. Now let B be the random variable for connections across two time steps [as in (8)], and let $\langle B(i,i,t)\rangle \equiv q'$, etc. Then from equations of the form

$$\begin{aligned} 1 - B(i,i,t) = &\left[1 - A(i,i,t)A(i,i,t+1)\right] \\ &\times\left[1 - A(i,i+1,t)A(i+1,i,t+1)\right] \\ &\times\left[1 - A(i,i-1,t)A(i-1,i,t+1)\right] \end{aligned} \tag{31}$$

we get

$$\begin{aligned} 1 - q' &= (1-q^2)(1-r^2)^2(1-p^2)^2 \\ 1 - p' &= (1-pq)^2(1-pr)^2 \\ 1 - r' &= (1-qr)^2(1-p^2) \end{aligned} \tag{32}$$

Equations (32) are exact. What needs to be noted, however, is that with two time steps there is also the possibility of a bond from A to J, and the parameter space (so far just q, p, and r) would have to be further extended if another scale transformation would be performed. A second scale transformation using only the parameters r', p', and q' would also neglect the fact that the new parameters are correlated. That is, for the original bonds, the probability of an A–D connection is p whether or not the A–B connection exists. Consider, however, the (conditional) probability for an A–H bond given that there is an A–F bond. The given information on the A–F bond increases the *a priori* probability for the existence of an A–C bond which in turn makes the A–H bond more likely. Thus the full parameter space after a single time step decimation includes not just q', p', and r' but a set of correlations and three- and four-step probabilities.

Equation (32) is of the general form

$$p_i' = F_i(p_0, \ldots, p_M), \qquad i = 0, \ldots, M \tag{33}$$

for nonlinear F_i. This transformation will be iterated, neglecting the necessity of expanding the parameter space on successive transformations.

The transformation has several fixed points which we designate $\mathbf{p} = (p_0, \ldots, p_M)$. First $\mathbf{p}^{(0)} = (0,0,0)$ ($M = 2$ in our case) indicates a completely unconnected lattice. For $\mathbf{p}^{(1)} = (1,1,1)$ the lattice is completely connected with an infinite percolating cluster. The point $\mathbf{p}^{(1')} = (1,0,1)$ is also a fixed point and indicates a lattice with an infinite percolating cluster. All the above are attractors. Numerically we find two other fixed points which are repellers: $\mathbf{p}^{(c)} = (0.34227, 0.30096, 0.22560)$ and $\mathbf{p}^{(c')} = (0.57430, 0, 0.45056)$.

To find p_c we take an initial condition $\mathbf{p} = (0, p, 0)$ and iterate. For $p < p_c$ the iteration leads to $\mathbf{p}^{(0)}$ while for $p > p_c$ the iteration should lead to one of the connected fixed points. (In fact it leads to $\mathbf{p}^{(1')}$. This will be discussed below.) Carrying out the foregoing scheme numerically leads to the following value for p_c:

$$p_c = 0.6317 \ldots \tag{34}$$

Next consider the critical exponent for the "time" correlation length, i.e.,

$$\xi(p) \sim \frac{1}{(p_c - p)^{\nu}} \tag{35}$$

for $p < p_c$ (our considerations apply as well to $p > p_c$). Using the usual renormalization group theory arguments we get

$$\nu = \frac{\log 2}{\log \lambda} \tag{36}$$

where λ is the largest eigenvalue of the matrix $\partial F_i / \partial p_j$ evaluated at the repelling critical value of $\mathbf{p}$.

For the problem at hand there is some question as to which repeller $\mathbf{p}^{(c)}$ or $\mathbf{p}^{(c')}$ should be used for the evaluation of λ. The initial condition $(0, p_c, 0)$ leads to $\mathbf{p}^{(c')}$ because of a special property of the transformation, namely, if ever p becomes zero it stays zero. For any initial condition $(0, p, 0)$ this happens on the first step. However, any slight perturbation, say, $(0, p, r)$ for very small r, sends the trajectory to $\mathbf{p}^{(c)}$ instead. Moreover, the critical point $\mathbf{p}^{(c')}$ has its own peculiarities: two eigenvalues of $\partial F_i / \partial p_j$ exceed 1. If $\mathbf{p}^{(c')}$ is the physical fixed point then the larger is nonphysical since it leads out of the set of values $(q, 0, r)$. The smaller eigenvalue at $\mathbf{p}^{(c')}$ leads to a critical exponent 1.50 (the larger eigenvalue would give 0.97). The critical exponent associated with $\mathbf{p}^{(c)}$ is $\nu = 1.25$.

The fact that small perturbations in the $(0, 1, 0)$ direction lead away from $\mathbf{p}^{(c')}$ might suggest that $\mathbf{p}^{(c)}$ is the physical fixed point. However, such perturbations do not occur. The first step from $(0, p, 0)$ to $(q, 0, r)$ is exact and on subsequent steps the neglected correlations would not, in fact, introduce any contribution proportional to $(0, 1, 0)$. Therefore, with three terms allowed ($M = 2$) we have

$$\nu = 1.5 \tag{37}$$

One can also expand the parameter space and we have looked at $M = 3$, 4, and 5. The value of p_c is unchanged for $M = 3$, because of the peculiar vanishing of p $(= p^{(1)})$ as well as $p^{(3)}$ on the second iteration. $M = 4$ and 5 give a value of p_c of about 0.571, which is considerably worse than 0.63 when compared to the values obtained from computer simulations. See our comments in Section 5 on this phenomenon. The critical

exponent for $M = 5$ from the smaller eigenvalue (but still greater than 1) near $\mathbf{p}^{(c')}$ is 1.25 and the nonzero elements of $\mathbf{p}^{(c')}$, namely, (p_0, p_2, p_4) appear to be equal to (p_0, p_1, p_2) of the $M = 2$ fixed point at $\mathbf{p}^{(c)}$.

The computer simulations give $p_c = 0.639 \pm 0.003$ and $\nu = 1.5 \pm 0.2$ for the region of $p < p_c$. For $p > p_c$ we obtain β and find $\beta = 0.31 \pm 0.05$ with $p_c = 0.644 \pm 0.001$. The values of p_c obtained above and below p_c seem to differ slightly but are in reasonable agreement with the calculated value ($\sim$2.5%). Mauldon[9] found a value for p_c of 0.630. We have not calculated β theoretically but we can compare our results with those of Blease.[10] From a series calculation he obtained $\beta = 0.28 \pm 0.02$, consistent with our value. From simulations we get $\gamma = 2.11 \pm 0.15$ (see ref. 10 for definition of γ).

The agreement between our theory and the numerical simulations is thus good both for p_c and for ν, provided one stops at $M = 3$ or 4 and takes $\mathbf{p}^{(c')}$ as the physical fixed point.

5. TWO-PLUS-ONE-DIMENSIONAL PERCOLATION

This is the case of astrophysical interest. As discussed in Section 2, we choose a two-dimensional triangular lattice. When the random variable σ_α takes the value 1 the site (or "cell") is said to be alive and in the astrophysical case corresponds to there being a bright young star (or stars) in the cell. The probability p is the probability that the supernova explosion of this bright star leads to the formation of a bright star (or stars) in an adjacent cell. In references 1–4 the rule used for generating the stochastic galaxy evolution is

$$\text{Prob}\left[\sigma_\alpha(t+1) = 1\right] = 1 - (1-p)^n \tag{38}$$

where n is the number of live neighbors of cell α. Equation (38) can be rewritten in terms of our previous notation as

$$\sigma_\alpha(t+1) = 1 - \prod_{\beta=1}^{6} \left[1 - A_{\alpha\beta t}\sigma_\beta(t)\right] \tag{39}$$

where β runs over the six neighbors of cell α at time t. To see that (38) follows from (39) take the expectation value of (39):

$$\langle \sigma_\alpha(t+1)\rangle = \text{Prob}\left[\sigma_\alpha(t+1) = 1\right] = 1 - \left\langle \prod_\beta \left[1 - A_{\alpha\beta t}\sigma_\beta(t)\right]\right\rangle \tag{40}$$

In (40) the expectation is only over the sample space associated with the A's. The configuration of the sigmas at time t is assumed given. Since the

A's are all independent (40) yields

$$\langle \sigma_\alpha(t+1)\rangle = 1 - \prod_\beta \left[1 - \langle A_{\alpha\beta t}\rangle \sigma_\beta(t)\right] = 1 - (1-p)^n \tag{41}$$

From (39) we make a mean field theory estimate of ρ, the density of living cells in the galaxy. Assuming *no* correlation between neighboring cells, we take an expectation of (39) in which the sigmas too are random variables. Thus

$$\rho(t) = \langle \sigma_\alpha(t)\rangle, \qquad \text{any } \alpha \tag{42}$$

(we neglect systematic spatial variation of ρ in the galaxy). The assumption that the sigmas are uncorrelated means that

$$\rho(t+1) = 1 - \left\langle \prod_{\beta=1}^{6} (1 - A_{\alpha\beta t}\sigma_\beta(t)) \right\rangle = 1 - \left[1 - p\rho(t)\right]^6 \tag{43}$$

A fixed point of (43) is an equilibrium density and the equation

$$\rho = 1 - (1 - \rho p)^6 \tag{44}$$

provides a function $\rho(p)$. As before, $\rho \equiv 0$ is a solution and for $p > 1/6$ there is a second solution which approaches 1 as p approaches 1. There can be no more than one solution in the real interval (0, 1). In Fig. 2 we show a graph of $\rho(p)$ with the solution of Eq. (44) marked as a solid line. Also shown are experimental points for densities of nonrotating galaxies taken

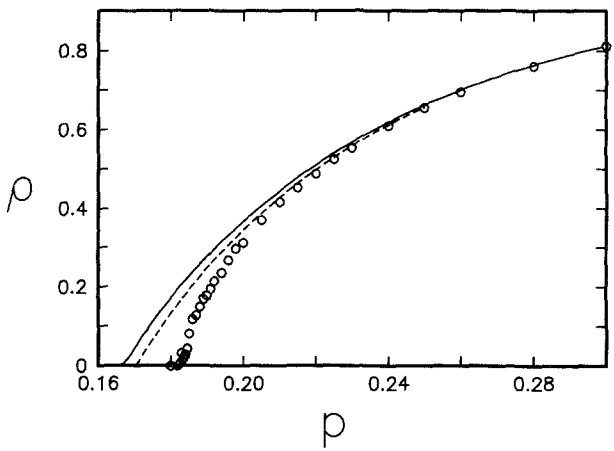

Fig. 2. The solid line is zeroth-order mean field theory, i.e., the solution $\rho(p)$ of Eq. (44). The dashed line just below it is $\rho(p)$ from Eqs. (50)–(53), a solution that includes the effect of lowest-order cumulants. The circles are the results of numerical simulations with zero rotational velocity.

from time averages of a number of stochastically evolving galaxy models. For $p > 0.22$ agreement is fairly good showing that even for p as close to the critical value as 0.22, correlations do not play a significant role.

However, experience with the galaxy models has shown that the formation of spiral arms most resembling those found in nature takes place for $0.02 < \rho < 0.1$. From the graph, these values of ρ are obtained for p much closer to critical than 0.22 and the lowest-order theory is therefore unsatisfactory. A further reason for believing the p regime in which correlations are significant to be the important regime for spiral arm formation is the dependence of density on shear (with given p). The density is in fact found to increase. This can be understood by noting that, whatever else shear does, it surely cuts down on the effect of correlations since it causes cells to be influenced by more distant cells than would be the case if there were no shear. This is consistent with Fig. 2 since the mean field ρ always lies above the experimental (correlated) ρ.

Before considering improvements to (43) we calculate from (44) a mean field critical exponent governing the extinction of ρ as $p \to 1/6$. For Eq. (44), p_c = (critical probability) = $1/6$. The critical exponent β is defined in Eq. (7). From (44) it is easy to show that

$$\rho = \tfrac{72}{5}(p - p_c) + O\big((p - p_c)^2\big), \qquad p > p_c \tag{45}$$

and β is therefore 1.

A first improvement to our theory includes the effect of two-cell correlations for nearby cells. Again take the expectation of (39), but now keeping two-cell cumulants [see Eqs. (24)–(26) and Ref. 8]

$$\begin{aligned}\rho(t+1) = \langle \sigma_\alpha(t+1)\rangle &= 1 - \left\langle \prod_{\beta=1}^{6} \big[1 - A_{\alpha\beta t}\sigma_\beta(t)\big] \right\rangle \\ &= 1 - (1-p\rho)^6 - (1-p\rho)^4 \\ &\quad \times \sum_{\text{pairs } \gamma,\delta} \big\langle \big[1 - A_{\alpha\gamma t}\sigma_\gamma(t)\big]\big[1 - A_{\alpha\delta t}\sigma_\delta(t)\big]\big\rangle_c \end{aligned} \tag{46}$$

where the subscript c stands for cumulant and the sum includes one contribution from each pair σ_γ and σ_δ ($\gamma \neq \delta$). ρ with no argument is $\rho(t)$. Since the A's are all independent we have

$$\big\langle \big[1 - A_{\alpha\gamma t}\sigma_\gamma(t)\big]\big[1 - A_{\alpha\delta t}\sigma_\delta(t)\big]\big\rangle_c = p^2 \langle \sigma_\gamma(t)\sigma_\delta(t)\rangle_c \tag{47}$$

It remains therefore to evaluate $\sum_{\text{pairs}} \langle \sigma_\gamma(t)\sigma_\delta(t)\rangle_c$. This is done, as in Schulman and Seiden,[8] by assuming that the correlations at time t are those arising through the evolution rules from an uncorrelated state at time $t-1$. In effect we are only looking at first-order terms in the cumulants. By

Eq. (39) and by the definition of cumulants

$$\langle \sigma_\gamma(t)\sigma_\delta(t)\rangle_c = \langle [1-\sigma_\gamma(t)][1-\sigma_\delta(t)]\rangle_c$$
$$= \left\langle \prod_{\psi=1}^{6} [1 - A_{\gamma\psi t-1}\sigma_\psi(t-1)] \prod_{\phi=1}^{6} [1 - A_{\delta\phi t-1}\sigma_\phi(t-1)] \right\rangle$$
$$- \left[\left\langle \prod_{\psi=1}^{6} [1 - A_{\alpha\psi t-1}\sigma_\psi(t-1)] \right\rangle \right]^2 \tag{48}$$

If the product over ψ and the product over ϕ had no common cells then with the neglect of cumulants at $t-1$ the cumulant on the left-hand side would be zero. So for given γ and δ we look for cells that appear in both the products over ψ and over ϕ. For such a cell, say, 0,

$$\langle [1 - A_{\gamma 0t-1}\sigma_0(t-1)][1 - A_{\delta 0t-1}\sigma_0(t-1)]\rangle$$
$$= 1 - 2p\rho(t-1) + p^2\langle \sigma_0^2(t-1)\rangle$$
$$= 1 - 2p\rho(t-1) + p^2\rho(t-1) \tag{49}$$

since $\sigma^2 = \sigma$. The correlation comes about because the coincident cell causes ρ to appear as the last term in the sum in (49), rather than ρ^2. If for a pair γ, δ there is a single coincident cell (among the six neighbors of each) then calling this cumulant S ("single"), we have

$$\langle \sigma_\gamma(t)\sigma_\delta(t)\rangle_c = S = (1-p\rho)^{10}\left[(1 - 2p\rho + p^2\rho) - (1-p\rho)^2\right] \tag{50}$$

the ρ's on the right being $\rho(t-1)$. Obviously

$$S = p^2\rho(1-\rho)(1-\rho p)^{10} \tag{51}$$

If γ and δ have two common neighboring cells, the cumulant will be designated D ("double") and

$$\langle \sigma_\gamma(t)\sigma_\delta(t)\rangle_c = D = (1-\rho p)^8\left[(1 - 2\rho p + \rho p^2)^2 - (1-\rho p)^4\right] \tag{52}$$

Next look to each pair in the product in Eq. (46) to count the number of pairs having 0, 1, 2 or more common cells. Figure 3 is a diagram of a cell and its neighbors. Cells are not actually drawn in the diagram, but rather

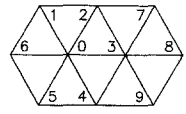

Fig. 3. Cells (vertices) and their neighbors.

the vertices represent cells. Letting α of Eq. (46) be 0, then the pairs are all pairs of the set $\{1,2,3,4,5,6\}$. Consider a pair of the sort 1-2. For purposes of checking their common neighbors, this is the same as looking at the pair 0-3. Among the neighbors of 0 and 3 exactly two are common, namely, 2 and 4. Hence the pairs 1-2, 2-3, 3-4, 4-5, 5-6, and 6-1 all contribute terms D to the sum over pairs in (46). A pair of the sort 1-3 also gives a contribution D since 1 and 3 have exactly 2 common neighbors (0 and 2). (When we wish to distinguish the two sorts of "double" cumulants, type 1-2 will be designated D and type 1-3, D'.) This gives 6 more D's: 1-3, 2-4, 3-5, 4-6, 5-1, 6-2. Finally, there are the pairs 1-4, 2-5, and 3-6 all of which obviously give S.

This is all the information needed to iterate the density. We summarize

$$\rho(t+1) = 1 - [1 - p\rho(t)]^6 - [1 - p\rho(t)]^4 p^2 (12D + 3S) \tag{53}$$

and D and S are given by (50)–(52) involving $\rho(t-1)$.

To find the equilibrium "equation of state" $\rho(p)$, all ρ's in (50)–(53) are set equal and the system solved. Again there is always the trivial solution $\rho = 0$. In Fig. 2 we also plot (the dashed line) the curve of nontrivial solutions $\rho(p)$ of the Eqs. (50)–(53). Although slight improvement can be noted, the theory clearly misses the mark. (The value of p_c given by this improved mean field theory is $p_c = 0.1704$, better than $1/6$, but still far from the "experimental" value of 0.183.)

Visual inspection of low-density galaxy models suggests the origin of the discrepancies. Living regions are patchy and isolated. There are large dead regions, which we shall call "vacuum." A vacuum area can only come alive through the invasion of life from other regions. Within the vacuum what is dead stays dead, and the probabilistic considerations given above are particularly inaccurate. Said otherwise, the formation of vacuum represents a very-high-order correlation.

Granted that the above theory does not well describe the vacuum, one can ask if it is accurate within the living regions. To this end we define a quantity ρ_L, local density, the density in the nonvacuum areas. A vacuum cell is defined as one that is dead and has no living neighbors. If the entire model galaxy has M cells of which L are living and V are vacuum, then

$$\rho_L = \frac{L}{M - V} \tag{54}$$

In terms of the statistical model this is

$$\rho_L = \frac{\rho}{1 - \left\langle \prod_{\alpha=0}^{6} (1 - \sigma_\alpha) \right\rangle} \tag{55}$$

the seven cells in the product being a cell (0) and its six neighbors. The product in (55) can be evaluated to second-order cumulants to give an expression

$$\frac{V}{M} = \left\langle \prod_{\alpha=0}^{6} (1-\sigma_\alpha) \right\rangle \cong (1-\rho)^7 + (1-\rho)^5 \sum_{\text{pairs}} \langle \sigma_\alpha \sigma_\beta \rangle_c$$
$$= (1-\rho)^7 + (1-\rho)^5 (18D + 3S) \tag{56}$$

The six additional D's in (56) [compared to (53)] arise from cumulants of the central cell with its neighbors.

In Fig. 4 experimental local densities are compared to the theoretical predictions. Evidently, even at the lowest (experimental) values of ρ (which correspond to $p \to p_c$) the theory is doing quite well on the local density. In fact, the lowest-order mean field theory (solid line in the figure) does not do too badly either.

It follows that an important defect in the mean field theory is the inadequate description of the vacuum. It is apparently the high-order correlations associated with vacuum that cut down the density, and presumably the effect of shear is the disruption of those correlations so as to allow increased density. In Section 6 we shall elaborate on the important effect that clumping both in the vacuum and in the living regions has on the formation of well-articulated spiral arms.

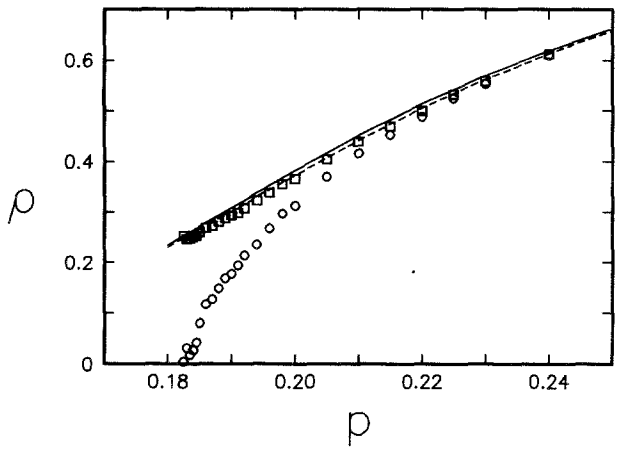

Fig. 4. Local densities. Curves are mean field theory predictions for local density with (dashed line) and without (solid line) lowest-order cumulants. Squares are experimental local densities. Experimental total density (circles) has also been plotted to bring out the extent to which exclusion of vacuum affects the density.

5.1. Scale Transformation

The scale transformation to be applied to our (2 + 1)-dimensional directed percolation problem is time step decimation. We define $B(\alpha, \beta, t)$ to be a random variable taking the value 1 if there is *some* path of forward directed bonds from site α at time t to site β at time $t + 2$, and zero otherwise. Therefore the following relation is exact

$$1 - B(\alpha, \beta, t) = \prod_{\gamma} \left[1 - A(\alpha, \gamma, t) A(\gamma, \beta, t + 1)\right] \tag{57}$$

In Eq. (57), α, β, and γ are not restricted to being nearest neighbors. Until now we have taken $A(\alpha, \beta, t)$ to be zero unless β was one of the six nearest neighbors of α, in which case it took the value 1 with probability p. (With shear some further variation was permitted, but for scale transformation considerations we shall only study the case of no shear.) Note though that if A is nonzero for nearest neighbors only, B no longer has that property. Since our intention is to iterate the transformation we must consider more elaborate connection rules. Each possible connection will have its own probability and we enlarge the parameter space from p to $\mathbf{p} = (p_0, p_1, \ldots, p_M)$ for various possible bonds $1, \ldots, M$ (to be defined below).

Clearly, no matter how large M, successive iteration of a relation of the sort (57) will eventually make the parameter space $(p_0, \ldots, p_M)$ inadequate. For this reason we deal with a truncated version of (57) in which some of the induced connections are discarded. A second effect that we neglect is the correlations among various B's resulting from their being built up from the A's. Thus (by definition) the A's are all independent random variables and $\langle A_{\alpha\beta t} A_{\alpha'\beta' t'} \rangle_c = 0$ so long as not all three indices (or arguments) are the same. By contrast, it is easy to see that

$$\langle B(0,2,0) B(0,0,0) \rangle_c = (1 - p^2)^4 \left\{ (1 - 2p^2 + p^3)^2 - (1 - p^4)^4 \right\} \neq 0 \tag{58}$$

where sites are labeled as in Fig. 3. In our scale transformations we shall also neglect these induced correlations.

In our calculations we have used from two to nine parameters. In Fig. 5 we indicate the cell–cell connections associated with the various parameters. To get all connections up to first-nearest neighbors p_0 and p_1 are needed; for second-nearest neighbors use p_0 to p_3; and so forth. As in other renormalization group type calculations, increasing the number of parameters need not improve results. In our case the source of this can be traced to the effect of neglected correlations.

The result of an iteration is to produce a set of parameters $\mathbf{p}' = (p_0', \ldots, p_M')$. The equation for the iteration is gotten from Eq. (57) by taking a particular pair of sites for which there is an associated parameter

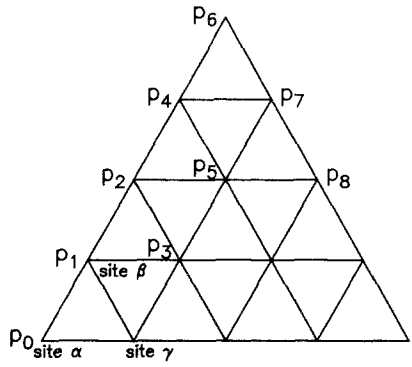

Fig. 5. Parameters for the probabilities of various site–site connections. Thus the probability that there is a connection from site α to itself on the next "time" step is p_0. The probability that there is a connection from site α to site β (or to site γ or from β to γ) on the next time step is p_1.

in the parameter set and evaluating the expectation of "B" for that pair by allowing all possible intermediate sites in the product and neglecting correlations. Newly generated nonzero probabilities for pairs of sites out of the parameter set are dropped. For example, suppose we are restricted to first-nearest neighbors only, so $\mathbf{p} = (p_0, p_1)$. Then the scaled probability for a site to be connected to itself (on the next, scaled, time step) is

$$p_0' = 1 - (1 - p_0^2)(1 - p_1^2)^6 \tag{59}$$

Similarly, the scaled nearest neighbor probability is

$$p_1' = 1 - (1 - p_0 p_1)^2 (1 - p_1^2)^2 \tag{60}$$

For this transformation there are two obvious fixed points: $\mathbf{p}^{(0)} = (0, 0)$ and $\mathbf{p}^{(1)} = (1, 1)$ representing completely disconnected and connected (three-dimensional) lattices, respectively. The critical fixed point is $\mathbf{p}^{(c)} \cong (0.330141, 0.215488)$ and this is reached for an initial vector $\mathbf{p}_{\text{in}} \cong (0, 0.308158)$ so that $p_c \cong 0.308$ (which is large compared to the computer simulation value of 0.183 given in Table I).

The critical exponent for the correlation length in the time direction is obtained as in Eqs. (35) and (36), where λ is the largest eigenvalue of $\partial F_i / \partial p_j$ evaluated at $\mathbf{p}^{(c)}$ and F_i is defined as in Eq. (33). The value of ν from the iteration rule (59)–(60) is

$$\nu = 1.20$$

Consider next scale transformations involving more parameters. To facilitate the writing of these transformations we introduce the following

Table I. Critical Parameters from Simulation Experiments for the Case of 2 + 1 Dimensions.

Shear [a]	From $p < p_c$ data		From $p > p_c$ data	
	p_c	ν	p_c	β
0	0.1830 ± 0.0012	1.13 ± 0.11	0.1831 ± 0.0004	0.65 ± 0.06
0.1	0.1815	1.12		
0.2	0.1798	1.10		
0.4	0.1791	1.09	0.1792	0.66
1.0	0.1757	1.07		
10	0.1719	1.04	0.1730	0.69

[a] With no shear we get $\gamma = 1.50 \pm 0.10$ (see Blease[10] for definition of γ).

notation

$$R(i, j) = 1 - p_i p_j \tag{61}$$

The iteration rule will be written as

$$p_l' = 1 - \prod_{i,j} R(i, j)^{K_l(i,j)} \tag{62}$$

where the product is over i and j but with $j \leqslant i$, so that each possible pair appears exactly once. The transformation is then specified through the exponents $K_l(i, j)$ which are given in Table II. For the scale transformation involving k parameters ($k = 2$, 4, 6, or 9) truncate the matrices $K_l(i, j)$ to those in which only entries with $l, i, j \leqslant k$ are included.

For each of these scale transformations there is a pair of trivial fixed points: ($p_i = 0$, all i) and ($p_i = 1$, all i). In addition there is a critical fixed point and an associated largest eigenvalue of the transformation. In Table III we list the fixed point and the value of ν associated with the eigenvector and eigenvalue in accordance with Eq. (36). For each of these there is a value of p (the original probability of nearest-neighbor connection when no other connections are allowed) which we call p_c such that for $p < p_c$ and $\mathbf{p}_{\text{initial}} = (0, p, \ldots)$ the iteration leads to $(0, 0, \ldots)$ and for $p > p_c$, $(0, p, 0, \ldots)$ leads to $(1, 1, \ldots)$. For an initial vector $(0, p_c, 0, \ldots)$ the iteration leads to the vector $\mathbf{p}^{(c)}$.

The simulation results are shown in the first line of Table I. Observe that the best agreement between theory and simulation occurs using nine parameters in the calculation of p_c, but better values for ν are predicted when fewer parameters are used, namely, 4 or even 2. This is, in fact, a reasonable situation. It can be shown[11] that with the neglect of correlations produced by scaling, the fixed point necessarily has $\nu = 1$. Hence for the calculation of ν one does not wish to enlarge the parameter space to the point where correlations become very important. There is, of course, the embarrassment that without the simulation data one would not know where

Table II. Exponents of the Factors $(1 - p_i p_j)$ Entering the Scale Transformation. Listed Below Is the Array $K_l(i, j)$ of Eq. (62). Only the Diagonal and Upper Triangle Are Used. Blank Entries Are Zero

$l = 0$

	0	1	2	3	4	5	6	7	8
0	1								
1		6							
2			6						
3				6					
4					6				
5						12			
6							6		
7								12	
8									6

$l = 1$

	0	1	2	3	4	5	6	7	8
0		2							
1		2	2	4					
2				4	2	4			
3						4			
4						4	4	4	
5						2		4	4
6								4	
7									4
8									

$l = 2$

	0	1	2	3	4	5	6	7	8
0			2						
1		1		4	2	4			
2			2				2		4
3						4		4	
4						4			
5								4	
6									4
7								2	
8									

$l = 3$

	0	1	2	3	4	5	6	7	8
0			2						
1		2	4			4			
2						4		4	
3				2	4				2
4									4
5						2	4	4	
6									
7								2	
8									

$l = 4$

	0	1	2	3	4	5	6	7	8
0					2				
1			2			4	2	4	
2						4			
3				2					4
4					2				
5								4	
6								4	
7									
8									

$l = 5$

	0	1	2	3	4	5	6	7	8
0						2			
1			2	2	2	2		2	2
2				2	2			2	
3						2	2	2	
4								2	
5						2	2		2
6									
7									2
8									

$l = 6$

	0	1	2	3	4	5	6	7	8
0						2			
1			2		4				
2		1							4
3				4					
4					4				
5				2					
6					2				
7									
8									

$l = 7$

	0	1	2	3	4	5	6	7	8
0								2	
1					2	2	2		2
2				2		2		2	
3						2		2	
4						2	2		
5									2
6									
7								2	
8									

$l = 8$

	0	1	2	3	4	5	6	7	8
0									2
1						4		4	
2			2				4		
3				1	4				
4									
5						2		4	
6									
7									
8									2

to stop enlarging the parameter space for ν and how far to continue for p_c. This is, in fact, a general problem of the renormalization group method and it is known that enlarging the coordinate space may worsen results. Note that as the shear increases, ν does decrease toward unity. The effective long-range interaction induced by shear explains this. As for the case of 1 + 1 dimension, Blease[10] has calculated β and finds 0.60 ± 0.05, in good agreement with our result. Interestingly, we find β to be close to $(d - 1)/d$

Table III. Critical Properties for Various-Size Parameter Space. $\mathbf{p}^{(c)}$ Is the Critical Repeller. k Is the Number of Parameters Used, p_c Is the Value of the Initial Nearest-Neighbor Connection Probability Needed to Hit $\mathbf{p}^{(c)}$ Under the Iteration. ν Is as Given in Eq. (36).

k	p_c	ν	$\mathbf{p}^{(c)}$
2	0.308	1.20	(0.33014, 0.21549)
4	0.207	1.09	(0.12602, 0.10253, 0.06206, 0.07307)
6	0.1886	1.04	(0.06527, 0.05753, 0.04395, 0.04750, 0.02802, 0.03350)
9	0.1804	1.01	(0.03972, 0.03637, 0.03060, 0.03203, 0.02334, 0.02578, 0.01576, 0.01864, 0.01968)

for 2 + 1 dimensions which is the value suggested by some rather heuristic arguments of Shante and Kirkpatrick.[12]

5.2. Effect of Shear

Before doing a detailed calculation a few qualitative remarks are in order. It is shear that lies behind the stable arm morphology in galaxies in two distinct ways. First there is a simple kinematic effect. Just as a gob of dark-colored dough in a light batter will elongate and spiral as the dough is mixed, so a patch of living cells will be drawn into a spiral shape. The fact that the system is near a phase transition enhances this effect since the long correlation lengths near criticality tend to enlarge the "patches" of living cells. However, there is another important effect. The shifts (changing of neighbors) due to the shear give rise to increased production of stars at the sites of the shifts. That this is so can be seen from comparison of the mean field and exact (experimental) functions $\rho(p)$. From Fig. 2 it is clear that for small ρ correlations play an important role in cutting down the number of stars. The shifts due to shear destroy some of these correlations and hence enhance "fertility." A direct way to see this is to consider the expected number of descendents of two living cells distant from each other and from all other living cells. The expected number is $12p$. By contrast, it is easy to show that for adjacent cells this expectation value is $12p - 2p^2$, cutting down fertility. Shear, therefore, by spreading the clumps of stars that tend to develop for p near p_c, enhances fertility and an increased number of stars may be expected to appear along the shift lines.

We have observed that spiral structure is most pronounced for $\rho \lesssim 0.1$, which requires p near p_c and large correlations and clumping. For this reason it appears that the second consideration given above is important in establishing galactic morphology. Keeping second-order cumulants, as in

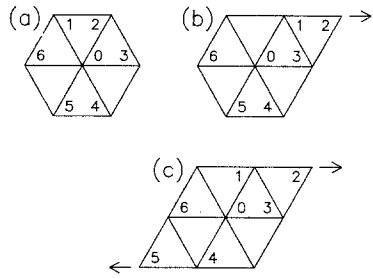

Fig. 6. (a) Cells at time $t + 2$ and, for the case of no slippage, at time $t + 1$ also. (b) Cells at time $t + 1$ for single slippage, as indicated by arrow. (c) Cells at time $t + 1$ for double slippage.

Eq. (46), the density at time $t + 2$ is given by

$$\rho(t+2) = \langle \sigma_0(t+2) \rangle = 1 - \left\langle \prod_{j=1}^{6} \left[1 - A_{j0t+1} \sigma_j(t+1) \right] \right\rangle$$

$$= 1 - \left[1 - p\rho(t+1) \right]^6 - \left[1 - p\rho(t+1) \right]^4$$

$$\times p^2 \sum_{\text{pairs}} \langle \sigma_i(t+1) \sigma_j(t+1) \rangle_c \tag{63}$$

where the cell numbering is given in Fig. 6a. As in the no-shear calculation, cumulants at time $t + 1$ arise from the configuration at time t and we shall calculate them as if the time t configuration were of density $\rho(t)$ but without correlations. However, for a given pair entering the sum in (63) the kind of cumulant that it contributes (D or S, etc.) will depend on the time t configuration, which in turn depends on whether there has been a shift. For example, with no shift, the 2-4 pair yields a D (double) cumulant, while with a single shift (cf. Fig. 6b) it is only an S (single) cumulant. With two shifts (Fig. 6c) there is even greater change. In Table IV is a list of pairs and the kind of cumulant associated with each pair in the case of 0, 1, or 2 shifts. Adding the contributions in the table and recalling that in fact D and D' are equal yields

$$\sum_{\text{pairs}} \langle \sigma_i \sigma_j \rangle_c = \begin{cases} 12D + 3S & \text{(no slip)} \\ 10D + 3S & \text{(one slip)} \\ 8D + 2S & \text{(two slips)} \end{cases} \tag{64}$$

The foregoing takes into account shifts taking place at time step $t + 1$ and the effect of these shifts in determining which cumulants enter the sum

Table IV. Pairs and Associated Cumulants. D and S Are Defined in Eqs. (50) and (52). A Distinction Is Made Between D's Arising from Pairs of Adjacent Cells and Those From Cells at Opposite Sides of a Rhombus. The Latter Are Primed, but Their Numerical Value in our Calculations Is Exactly the Same as That of D. X Indicates No Cumulant to This Order.

Pair	No slip	One slip	Two slips
1-2	D	D	D
1-3	D'	D	D
1-4	S	D'	S
1-5	D'	S	X
1-6	D	D'	D'
2-3	D	D	D
2-4	D'	S	X
2-5	S	X	X
2-6	D'	X	X
3-4	D	D	D'
3-5	D'	D'	X
3-6	S	S	S
4-5	D	D	D
4-6	D'	D'	D
5-6	D	D	D

in (63). A shift at time step t operates differently: It interferes with the building of the cumulants. Consider a cumulant of type D' (cf. Table IV), namely, $\langle \sigma_1 \sigma_2 \rangle_c$ of Fig. 7. This was calculated earlier by assuming no correlations at time t but by taking into account repetitions of the same site variable. Hence without shift, the two common neighbors of 1 and 2, namely, 3 and 9, give rise to a "double" cumulant [cf. Eq. (52)]. Suppose, however, that a shift took place at time t as indicated by the arrows (the time $t + 1$ configuration is shown in the figure). Then the neighbors of 1 at time t were sites 3, 4, 5, 6 (as before) and 7 and 8. The neighbors of 2 were

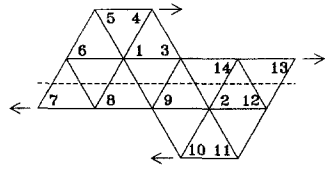

Fig. 7. Time $t + 1$ site labels. Arrows indicate direction of shift that took place at time t, so that site 8 was at the $t + 1$ position of site 9. Shift may be thought of as occurring along the dotted line.

9, 10, 11, 12 (as before) and 13 and 14. Hence in the product

$$\langle \sigma_1 \sigma_2 \rangle = \left\langle \left\{ 1 - \prod_{\alpha \in R_1} \left[1 - A_{1\alpha t} \sigma_\alpha(t) \right] \right\} \left\{ 1 - \prod_{\beta \in R_2} \left[1 - A_{2\beta r} \sigma_\beta(t) \right] \right\} \right\rangle$$

there are no common sites and the cumulant in this approximation is zero.

To calculate the total effect of shifts on the buildup of cumulants (in this approximation) one must go through Table IV entry by entry. Not all D' cumulants are affected in the same way as that described above. For example, with the same shift direction, $\langle \sigma_8 \sigma_3 \rangle_c$ (site labels of Fig. 7) simply changes from D' to D. On the other hand, $\langle \sigma_4 \sigma_9 \rangle_c$ becomes an S-type cumulant. D-type cumulants either are unchanged or become type D'—in either case taking the same value in this approximation. In Table V we show the changed cumulants for each pair for the shift pictured in Fig. 8. The net effect of the shift therefore is $D' \to S$ twice, $D' \to 0$ once, $S \to 0$ once, $S \to D$ once and $D' \to D$ once.

The two effects we have just discussed, that is, the changes in the cumulant terms due to shear, will be used in Eq. (71) below.

In our calculations for ρ when cumulants were needed we used a lowest-order approximation for those cumulants that neglected correlations in the buildup of the cumulants. That this severly underestimates the cumulants close to p_c can be seen from the poor agreement of $\rho(p)$ with

Table V. Each Cumulant $\langle \sigma_i \sigma_j \rangle_c$ Is Labeled by the Pair ij (in Column 1), the Labels Corresponding to the Time $t + 1$ Diagram of Fig. 8. Column 2 Gives the No-Shift Cumulant Type for That Pair and the Third Column Gives the Cumulant Type with Shift.

Pair	No shift	Shift
1-2	D	D
1-3	D'	S
1-4	S	Vanish
1-5	D'	Vanish
1-6	D	D
2-3	D	D
2-4	D'	D'
2-5	S	S
2-6	D'	D
3-4	D	D
3-5	D'	D'
3-6	S	D
4-5	D	D
4-6	D'	S
5-6	D	D

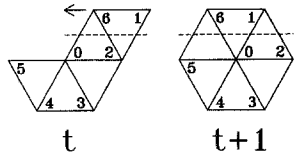

Fig. 8. Labels for shift at time step t. Arrow indicates direction of shift. Shift may be thought of as occurring along the dotted line.

simulation results very near p_c. Since the major effect of shear as so far described is expressed through cumulants (their substitutions and suppressions), it is clear that we shall require more accurate values for them near the critical point.

Our approach to estimating the size of the cumulants will be empirical and what will result is a one-parameter fit for the dependence of p_c on shear, that parameter being the value of p_c at zero shear. The latter quantity will be independently ascertained below both numerically and theoretically.

The basic, exact equation of motion is Eq. (39) and in Eq. (40) we looked at its cumulant expansion to a certain low order. Consider the exact cumulant expansion of Eq. (39):

$$\begin{aligned}\langle \sigma_\alpha(t+1)\rangle = {} & 1-\left[1-p\langle\sigma_\alpha(t)\rangle\right]^6-\left[1-p\langle\sigma_\alpha(t)\rangle\right]^4 \\ & \times \sum_{\substack{\text{pairs}\\ \gamma,\delta}} \left\langle\left[1-p\sigma_\gamma(t)\right]\left[1-p\sigma_\delta(t)\right]\right\rangle_c-\left[1-p\langle\sigma_\alpha(t)\rangle\right]^3 \\ & \times \sum_{\substack{\text{triples}\\ \gamma,\delta,\epsilon}} \left\langle\left[1-p\sigma_\gamma(t)\right]\left[1-p\sigma_\delta(t)\right]\left[1-p\sigma_\epsilon(t)\right]\right\rangle_c \\ & -(\text{cumulants of 4, 5, and 6 factors}) \\ & -\left[1-p\langle\sigma_\alpha(t)\rangle\right]^2 \sum_{\substack{\text{pairs } \gamma,\delta\\ \text{pairs } \epsilon,\zeta}} \left\langle\left[1-p\sigma_\gamma(t)\right]\left[1-p\sigma_\delta(t)\right]\right\rangle_c \\ & \times \left\langle\left[1-p\sigma_\epsilon(t)\right]\left[1-p\sigma_\zeta(t)\right]\right\rangle_c \\ & -(\text{other terms involving products of cumulants}) \end{aligned} \tag{65}$$

where the pairs γ,δ are appropriate neighbors of α, and similarly for the triples. When two pairs of pairs are taken they run over all possible distinct pairs of neighbors of α and similarly for other product terms. More on this expansion is given in Schulman and Seiden.[8] Both $\langle\sigma_\alpha(t+1)\rangle$ and $\langle\sigma_\alpha(t)\rangle$ can be replaced by ρ since we are interested in the equilibrium situation. Expressions such as $\langle\sigma_\gamma\sigma_\delta\rangle_c$ will be taken to refer to appropriate

neighbors of some particular site α at the same time t, although α and t will now be dropped from the notation. With the expansion of various products (65) becomes

$$\begin{aligned}\rho = {} & 6p\rho - 15p^2\rho^2 + O(\rho^3) \\ & - (1-p\rho)^4 p^2 \sum_{\substack{\text{pairs} \\ \gamma,\delta}} \langle \sigma_\gamma \sigma_\delta \rangle_c + (1-p\rho)^3 p^3 \sum_{\substack{\text{triples} \\ \gamma,\delta,\epsilon}} \langle \sigma_\gamma \sigma_\delta \sigma_\epsilon \rangle_c \\ & - \cdots - (1-p\rho)^2 p^4 \sum_{\substack{\text{pairs } \gamma,\delta \\ \text{pairs } \epsilon,\zeta}} \langle \sigma_\gamma \sigma_\delta \rangle_c \langle \sigma_\epsilon \sigma_\zeta \rangle_c - \cdots \end{aligned} \tag{66}$$

For p approaching p_c from above the behavior of ρ is given by

$$\rho \sim (p - p_c)^\beta \tag{67}$$

In examining (66) for leading behavior as $p \to p_c$ we do not have any *a priori* knowledge of the behavior of the cumulants. From simulation results we know, however, that they cannot all approach zero more rapidly than ρ [as given by (67)] for otherwise (66) would reduce to

$$(6p - 1)\rho = o(\rho)$$

yielding $p_c = 1/6$, exactly, which is incorrect. On the other hand, the cumulants cannot go to zero more slowly than ρ, for consider, for example, a two-site cumulant

$$\left| \langle \sigma_\gamma \sigma_\delta \rangle_c \right| \leqslant \langle \sigma_\gamma \sigma_\delta \rangle + \langle \sigma_\gamma \rangle \langle \sigma_\delta \rangle = O(\langle \sigma_\gamma \sigma_\delta \rangle) \leqslant O(\langle \sigma_\gamma \rangle) = O(\rho)$$

The first-order relation follows because $\langle \sigma_\gamma \rangle \langle \sigma_\delta \rangle = \rho^2$ and therefore vanishes faster than the cumulant. Hence it necessarily vanishes faster than the expectation of the product. The second order inequality follows by replacing σ_δ by 1 always, which must not decrease the value of the expectation. It follows then that at least some cumulants are $O((p - p_c)^\beta)$. In (66) we can therefore drop terms involving products of cumulants as well as ρ^2 terms to yield

$$\begin{aligned}(6p - 1)\rho = {} & p^2 \sum_{\substack{\text{pairs} \\ \gamma,\delta}} \langle \sigma_\gamma \sigma_\delta \rangle_c - p^3 \sum_{\substack{\text{triples} \\ \gamma,\delta,\epsilon}} \langle \sigma_\gamma \sigma_\delta \sigma_c \rangle_c \\ & + (\text{cumulants for 4, 5, and 6 sites}) \end{aligned} \tag{68}$$

To $O(\rho)$ Eq. (68) is exact. We now assume that two-site cumulants are larger than three- (and higher) site cumulants. In the Appendix we give a lowest-order calculation for a three-site cumulant and find it to be smaller than two-site cumulants by a factor p. Although we do not expect the expression derived there to hold near p_c it seems reasonable to suppose that

whatever values two- and three-site cumulants do take, the two-site cumulants will be somewhat larger. We therefore neglect all but two-site cumulants in (68) to obtain

$$\sum_{\substack{\text{pairs} \\ \gamma,\delta}} \langle \sigma_\gamma \sigma_\delta \rangle_c = \frac{6p_c - 1}{p_c^2} \rho \tag{69}$$

where p has been replaced by p_c, permissible to leading order.

The above considerations are valid with or without shear. We next introduce a parameter w to characterize the shear or shifting of cells past one another. All terms in Eq. (69) will then be treated as functions of w and we shall obtain the dependence of p_c on w. The parameter w is defined as the amount one row shifts past the adjacent row, measured in units of cell size. Thus, if $x_{ij}(t)$ is the x coordinate of cell (i, j) [= (row, column)] at time t then

$$w = \frac{\left[x_{i+1\,j}(t+1) - x_{i+1\,j}(t)\right] - \left[x_{ij}(t+1) - x_{ij}(t)\right]}{\left[x_{i\,j+1}(t) - x_{ij}(t)\right]} \tag{70}$$

The shear as defined in (70) is independent of i and j and in fact all bracketed difference quantities appearing are independent of i and j. Periodic boundary conditions are used throughout.

To study $p_c(w)$ we rewrite Eq. (69) (which holds for any w) as

$$\frac{p_c(w) - 1/6}{p_c(w)^2} = \frac{1}{6\rho} \sum_{\substack{\text{pairs} \\ (w)}} \langle \sigma_\gamma \sigma_\delta \rangle_c^{(w)} \tag{71}$$

The right-hand side of (71) has w written in two places, to emphasize that two effects are involved. First, with shear the pairs entering the sum change, and second the cumulants themselves are changed in value (reduced, presumably) because of the shift. These effects were derived above and we summarize them for the case of a single shift around some given cell:

$$\text{change in sum:} \qquad 6D + 6D' + 3S \rightarrow 6D + 4D' + 3S \tag{72}$$

$$\text{change in cumulants:} \qquad 6D + 6D' + 3S \rightarrow 8D + 2D' + 3S \tag{73}$$

where the meaning of (73) is that the cumulants that enter the sum were built up on the previous generation as if they were of the sort indicated on the right-hand side of the arrow.

The sum in (71) is an average over the entire lattice and it is convenient to take a probabilistic approach to the shifts. Specifically to first order in w there are $2wN$ shifts per time step, where N is the total number of cells in the system. The 2 arises because for each slippage two cells are involved (marriage and divorce statistics are sometimes clouded by the

same factor of 2). Consequently, to first order in w, Eq. (71) becomes

$$6\rho \frac{p_c(w) - 1/6}{p_c(w)^2} = (1 - 4w)(6D + 6D' + 3S) + 2w\left[(6D + 4D' + 3S) + (8D + 2D' + 3S)\right] \quad (74)$$

Second-order effects would include a single cell having a shift on both sides as well as shifts on two successive generations. A further approximation inherent in (74) is the use of (73) to describe the effect of shear on cumulants, as if their values (in particular the values of those involved in the shift) were built in a single time step. In addition we have the implicit assumption that the critical exponent β is independent of w, which is likely to be accurate for small w.[3]

For Eq. (74) to be useful we need information on the relative size of D, D', and S. Now these quantities were calculated to lowest order above [Eqs. (51) and (52) with $D' = D$] but the result is known to be an underestimate. However, it seems reasonable to suppose that although the magnitudes are incorrect the relative sizes for $p \to p_c$ are given by (51) and (52). With this ansatz it follows that

$$\begin{aligned} D &\sim 2S \\ D' &\sim 2S \end{aligned} \quad (75)$$

and we also assume these relations to be independent of w to lowest order in w. Equation (74) for $w = 0$ yields

$$S = \frac{6\rho\left[p_c(0) - 1/6\right]}{27 p_c(0)^2} \quad (76)$$

With (75) and (76), Eq. (74) can be rewritten entirely in terms of S and hence in terms of $p_c(0)$. Taking the derivative with respect to w [and using the notation $p_c(0) - 1/6 = \Delta p$] gives

$$\frac{1}{\Delta p} \frac{dp_c(w)}{dw} = -\frac{16}{27} \frac{1}{1 - (2\Delta p / p_c(0))}$$

Using the data in Table I, $p_c(0) \sim 0.183$, and therefore we have the prediction

$$\frac{dp_c}{dw} = -0.012$$

[3] $w = 0$ and $w = \infty$ are in different universality classes since the latter is a cross between $1 + 1$ and $\infty + 1$ percolation. We expect, however, that β does not depend strongly on w for small w.

This is in agreement with the value -0.015 obtained from Table I for a shear of 0.1.

We can see in Table I that p_c decreases appreciably with shear. For the largest shear, where $2/3$ of the correlations are completely destroyed (the correlations with cells in adjacent rings), p_c moves $2/3$ of the way from the zero shear result toward the mean field result $(1/6)$. As previously discussed in Section 2.1, ν decreases slowly toward unity, however, β remains roughly the same.

6. SUMMARY AND CONCLUSIONS

Stochastic star formation theories of galactic evolution take the radical view of neglecting detailed dynamical considerations and treating star formation probabilistically. In this paper we handle the Markov process that arises thereby as a problem in directed percolation. The case of primary physical interest—for the purpose of describing disk galaxies with their commonly occurring spiral arms—is percolation in three dimensions. The lattice is $\mathbf{L} \times \mathbf{Z}$ where $\mathbf{L}$ is a two-dimensional triangular lattice and the integers $\mathbf{Z}$ represent time. Bonds may lead from a site $\alpha \in \mathbf{L}$ at some $t \in \mathbf{Z}$ to $\beta \in \mathbf{L}$ at $t + 1 \in \mathbf{Z}$ where β is one of the six nearest neighbors of α. Such bonds exist with probability p and we find (numerically) the critical probability for percolation on this system to be $p_c = 0.1830 \pm 0.0012$. The critical index for cluster duration (i.e., for ξ the correlation length in the t direction, $\xi \sim |p_c - p|^{-\nu}$) is $\nu = 1.13 \pm 0.11$. For the percolation probability (which we call ρ because of its interpretation as star density) $\rho \sim (p - p_c)^{\beta}$ and we find $\beta = 0.65 \pm 0.06$. (See below for γ.) Away from the critical region mean field theory gives a rather good accounting for ρ; see Fig. 2. Moreover, even in the critical region mean field theory using first-order cumulants can give a good description of less-sensitive quantities, such as local density; see Fig. 4. This implies that the onset of the phase transition (from high p) is characterized by the growth of large regions of vacuum. In the critical regions we use renormalization group scale transformations (time step decimation) to get a value of ν within experimental error. This method also gives a value of p_c.

For astrophysical purposes, namely, the description of rotation in the galaxy, it is desirable to consider a variation of the bond connection rule. The bonds from a site α do not always go to the nearest neighbors of α, but rather with some probability w go to more distant neighbors. The quantity w is related to the galactic differential rotation rate since with differential rotation an exploding supernova can induce star formation in relatively distant gas clouds brought near to it by the rotation. Our theoretical description gives a good estimate of the extent to which differential rotation reduces p_c and makes it closer to the mean field value.

The consequences of this model for astrophysics and, in particular, the ramifications of the association with phase transitions have been discussed in earlier publications.[1–4] We here comment only on the most graphic of these consequences, the appearance of well-demarcated spiral arms in many disk galaxies. (See Ref. 5 for another view of spiral arm morphology.)

The proximity of the phase transition lies behind this morphology in a number of ways. First the long correlation lengths characteristic of second-order phase transitions lead to clumping even in relatively sparse systems so that galactic rotation can spread these large clumps into arms. Moreover, in addition to the clumping of the stars, there is the tendency for large clumpy regions of vacuum to develop (this follows from the successful calculation of the *local* density). When the galaxy rotates (differentially) the vacuum stretches too, providing the spaces necessary for the spiral arms to be well articulated. It also happens that this same clumpiness tends to cut down the expected number of progeny of any given living star so the fact that rotation reduces correlations (by displacing cells from their neighbors) means enhanced star formation along the slip lines in the cellular rotation. Finally, we note that another phenomenon familiar in phase transition work—critical slowing down—plays a role in the feedback mechanism described in our earlier work.[4] Not only does the feedback mechanism tend to send p to its critical value, but when p is in that range it will stay there longer, so that in observing a collection of galaxies one is more likely to come across those in the critical region.

Two other percolation problems are studied although they are not of relevance to the stochastic star formation model.

Directed percolation in the plane (what we call $1 + 1$ dimensions) can be defined on the integer points of the plane with bonds allowed to go from a point (i, j) to $(i + 1, j + 1)$ and $(i - 1, j + 1)$. Computer simulation gives $p_c = 0.640 \pm 0.005$ and critical indices $\nu = 1.5 \pm 0.2$, $\beta = 0.31 \pm 0.05$. (See below for γ.) Time step decimation gives quite good agreement with p_c and ν if one stops enlarging the parameter space at a judicious stage.

What we call $(\infty + 1)$-dimensional percolation considers the set $\{1, 2, \ldots, N\}$ and a discrete time axes, with bonds going from any i to any j at the next time step. Bonds have probability $p = x/N$ and the limit $N \to \infty$ is studied. The critical value is $x_c = 1$ and several properties of this system are calculated; in particular the decimation transformation is rigorously exact so that this model serves as an example for our other calculations.

APPENDIX. THREE-SITE CUMULANTS

Consider three different random variables X_1, X_2, and X_3 each of which is the product of other random variables $Y_{i\alpha}$, $\alpha \in K_i$ where K_i is an

index set and $i = 1, 2, 3$. Thus

$$X_i = \prod_{\alpha \in K_i} Y_{i\alpha} \tag{A.1}$$

For given i the $Y_{i\alpha}$ are distinct and independent but for different i they may not be independent.

[For the galaxy problem $X_i = 1 - \sigma_i(t)$ and $Y_{i\alpha} = 1 - A_{i\alpha t-1}\sigma_\alpha(t-1)$.]

We wish to express the cumulant $\langle X_1X_2X_3\rangle_c$ in terms of the cumulants of the Y's. By the cumulant $\langle X_1X_2X_3\rangle_c$ we mean

$$\begin{aligned}\langle X_1X_2X_3\rangle_c = \langle X_1X_2X_3\rangle - \big[\langle X_1X_2\rangle\langle X_3\rangle + \text{permutations}\big] \\ + 2\langle X_1\rangle\langle X_2\rangle\langle X_3\rangle\end{aligned} \tag{A.2}$$

Brackets on the right are ordinary expectation values. The variables X_i are reexpressed in terms of $Y_{i\alpha}$ according to (A.1) and by the general expansion in the appendix of Schulman and Seiden[8] the various expectations in (A.2) can themselves be written in terms of cumulants of Y's, for example,

$$\langle X_1X_2X_3\rangle = \sum_{\mathcal{P}(L_{123})} \left\langle \prod_{(i,\alpha)\in M_1} Y_{i\alpha} \right\rangle \left\langle \prod_{(i,\alpha)\in M_2} Y_{i\alpha} \right\rangle_c \cdots \left\langle \prod_{(i,\alpha)\in M_n} Y_{i\alpha} \right\rangle_c \tag{A.3}$$

where the sum is over partitions of the set L_{123} defined by

$$L_{123} = \{(i,\alpha) \,|\, i = 1, 2, \text{and } 3,\ \alpha \in K_i\} \tag{A.4}$$

and $\mathcal{P}(A)$ indicates the set of partitions of the set A. Thus a partition of L_{123} is a family of sets M_ν such that M_ν is a subset of L_{123}, $\bigcup_{\nu=1}^{n} M_\nu = L_{123}$ and the M_ν are disjoint. The term $\langle X_1X_2\rangle\langle X_3\rangle$ is written

$$\langle X_1X_2\rangle\langle X_3\rangle = \left\{ \sum_{\mathcal{P}(L_{12})} \left\langle \prod_{M_1} Y_{i\alpha} \right\rangle_c \cdots \right\} \left\{ \sum_{\mathcal{P}(L_3)} \left\langle \prod_{M_1} Y_{i\alpha} \right\rangle_c \cdots \right\} \tag{A.5}$$

where L_{12} is defined as in (A.4) but i can only take the values 1 and 2. Similarly for L_3 i takes only the value 3.

When the sum in (A.5) is expanded it is a sum of products of cumulants and each term in the product again represents a partition of the set L_{123}. However, $\langle X_1X_2X_3\rangle$ and $\langle X_1X_2\rangle\langle X_3\rangle$ differ in that certain partitions of L_{123} appear in the sum for the former but not the latter. Specifically, any partition (and only those partitions) in which each set M_i contains either only variables with index $(3,\alpha)$ or only variables with indices $(1,\alpha)$ and $(2,\alpha')$ will appear in both sums. Thus if sets of the form $M = \{(1,\alpha),(2,\alpha'),(3,\alpha'')\}$ or $\tilde{M} = \{(1,\alpha),(3,\alpha'')\}$ are in a partition, then they will appear in the sum for $\langle X_1X_2X_3\rangle$ but not for $\langle X_1X_2\rangle\langle X_3\rangle$.

Consider a partition in which no element contains elements from more than one of L_1, L_2, and L_3. This partition will contribute to every term in the sum (A.2) and as a result (since it appears thrice with each sign) it will cancel. Similarly, partitions in which only L_1 and L_2 are mixed but L_3 is

kept separate appear once with each sign and therefore cancel (similarly for other permutations).

Consequently, the only terms which survive are those for which at least one set of the partition contains elements from all three sets L_1, L_2, and L_3 (for example, M, defined in the text above).

The cumulant can therefore be written

$$\langle X_1 X_2 X_3 \rangle_c = \sum_{\mathcal{P}'(L_{123})} \left\langle \prod_{M_1} Y_{i\alpha} \right\rangle_c \cdots \left\langle \prod_{M_n} Y_{i\alpha} \right\rangle_c \tag{A.6}$$

where the prime on $\mathcal{P}$ indicates nontrivial partitions of L_{123}, that is, those in which at least one subset M_i includes elements from all three subsets L_1, L_2, and L_3.

We now apply this result to the galaxy calculation. The starting point is the first part of Eq. (46):

$$\rho(t+1) = \langle \sigma_\alpha(t+1) \rangle = 1 - \left\langle \prod_{\beta=1}^{6} \left[1 - A_{\alpha\beta t} \sigma_\beta(t) \right] \right\rangle \tag{A.7}$$

In Eq. (46) the expectation is expanded to lowest order in two-site cumulants. By contrast the general cumulant expansion for a product of several independent random variables is

$$\langle U_1 U_2 \cdots U_N \rangle = \sum_{\substack{\text{all partitions} \\ \text{of } \{1, 2, \ldots, N\}}} \langle U_{\alpha_{11}} \cdots U_{\alpha_{1J_1}} \rangle_c \cdots \langle U_{\alpha_{p1}} \cdots U_{\alpha_{pJ_p}} \rangle_c \tag{A.8}$$

(see the appendix of Schulman and Seiden[8]). Thus there are negative contributions to (A.7) from three-site cumulants of the form

$$W = \left\langle \prod_{i=1}^{3} \left[1 - A_{\alpha\beta_i t} \sigma_{\beta_i}(t) \right] \right\rangle_c \prod_{i=1}^{3} \langle \left[1 - A_{\alpha\beta_i' t} \sigma_{\beta_i'}(t) \right] \rangle \tag{A.9}$$

where β_i, $i = 1, 2, 3$ are any set of three neighbors of the site α and β_i' are the other three sites. There are, of course, additional contributions involving squares of three-site cumulants and similar terms, but we shall neglect all but first powers of any cumulant involving two or more sites. By standard manipulations W becomes

$$\begin{aligned} W &= -p^3 \left[1 - p\rho(t) \right]^3 \langle \sigma_{\beta_1}(t) \sigma_{\beta_2}(t) \sigma_{\beta_3}(t) \rangle_c \\ &= +p^3 \left[1 - p\rho(t) \right]^3 \langle \left[1 - \sigma_{\beta_1}(t) \right] \left[1 - \sigma_{\beta_2}(t) \right] \left[1 - \sigma_{\beta_3}(t) \right] \rangle_c \end{aligned} \tag{A.10}$$

Each of the random variables $1 - \sigma_{\beta_i}(t)$ can be expressed as a product over the six neighbors of β_i at time $t - 1$ and we get an expression of the form (A.1), (A.2). Consequently, by (A.6) we are interested in partitions that involve neighbors of all three sites: β_1, β_2, and β_3. We next confine ourselves to the same level of precision that was used in deriving Eqs.

(49)–(52); that is, in expectations of products of $1 - A\sigma(t-1)$ (the Y's) all higher cumulants will be neglected except those arising from a coincidence of sites. Specifically, the only nonzero higher cumulants will be those for which a site selected as a neighbor of β_1 is the same as a site selected as a neighbor of β_2. Moreover, since "nontrivial partitions" must involve neighbors of all three sites the only contribution to W will come from products in which all three neighbors involve the very same site.

For β_1, β_2, and β_3 neighbors of a given site α, there is only one site which can satisfy the requirements for a nonzero W in this approximation, namely, the site α itself. Consequently,

$$\begin{aligned} W = {} & +p^3\big[1 - p\rho(t)\big]^3\big[1 - p\rho(t-1)\big]^{15} \\ & \times \big\langle \big[1 - A_{\beta_1 \alpha t-1}\sigma_\alpha(t-1)\big]\big[1 - A_{\beta_2 \alpha t-1}\sigma_\alpha(t-1)\big] \\ & \times \big[1 - A_{\beta_3 \alpha t-1}\sigma_\alpha(t-1)\big]\big\rangle_c \end{aligned} \tag{A.11}$$

There remain two problems: enumerate the possible subsets $\{\beta_1, \beta_2, \beta_3\}$ giving rise to contributions W, and for each of these to evaluate the three-site cumulant appearing in (A.11).

The enumeration is easy: any three of α's neighbors give such a term and all such terms are the same. Thus there are $\binom{6}{3} = 20$ such identical terms.

The cumulant itself is given by

$$\begin{aligned} & \big\langle \big[1 - A_{\beta_1 \alpha t-1}\sigma_\alpha(t-1)\big]\big[1 - A_{\beta_2 \alpha t-1}\sigma_\alpha(t-1)\big]\big[1 - A_{\beta_3 \alpha t-1}\sigma_\alpha(t-1)\big]\big\rangle_c \\ & \quad = -p^3\big\langle \sigma_\alpha(t-1)\sigma_\alpha(t-1)\sigma_\alpha(t-1)\big\rangle_c \\ & \quad = -p^3\big[\big\langle \sigma_\alpha(t-1)^3\big\rangle - 3\big\langle \sigma_\alpha(t-1)^2\big\rangle\big\langle \sigma_\alpha(t-1)\big\rangle + 2\big\langle \sigma_\alpha(t-1)\big\rangle^3\big] \\ & \quad = -p^3\big[\rho(t-1) - 3\rho(t-1)^2 + 2\rho(t-1)^3\big] \end{aligned} \tag{A.12}$$

where we have used $\sigma_\alpha^2 = \sigma_\alpha$. Notice that considerable care must be exercised in evaluating products inside cumulants and the three identical terms $\sigma_\alpha(t-1)$ are treated as distinct until they appear in ordinary expectation value brackets.

Extending the notation of Eqs. (48)–(52) it is convenient to define

$$\big\langle \sigma_\gamma(t)\sigma_\delta(t)\sigma_\epsilon(t)\big\rangle_c \equiv T \qquad (\text{"triple"}) \tag{A.13}$$

for a case where γ, δ, and ϵ have a single common neighbor. We have just shown that

$$T = +p^3\big[\rho - 3\rho^2 + 2\rho^3\big]\big[1 - p\rho\big]^{15} \tag{A.14}$$

(where the ρ's are evaluated at $t-1$ in our approximation, and

$$W = -p^3\big[1 - p\rho(t)\big]^3 T \tag{A.15}$$

It is of interest to write down the new iteration equation [analog of Eq. (53)] and the new equation for the equilibrium value of ρ. The iteration equation is

$$\rho(t+1) = 1 - [1 - p\rho(t)]^6 - [1 - p\rho(t)]^4 p^2(12D + 3S)$$

$$+ [1 - p\rho(t)]^3 p^3 20T \tag{A.16}$$

with S and D given by Eqs. (51) and (52) and T given by Eq. (A.14). The equilibrium value is found by setting $\rho(t+1) = \rho(t) = \rho(t-1) \equiv \rho$ in (A.16).

The effect of T turns out to be quite small. There is a slight shift in p_c gotten from (A.16) by finding that value of p for which a positive solution for ρ appears. For the case of S, D, and T all set to zero we have the familiar $p_c = 1/6$. Keeping S and D but setting T to zero gives $p_c = 0.170467$ (the root of $27p^4 - 6p + 1 = 0$). By including T also we get $p_c = 0.170377$ (the root of $-20p^6 + 27p^4 - 6p + 1 = 0$). Thus the main shift from the lowest mean field value is gotten from D and S with T only correcting this shift by about 2%. For this reason in the main text we have ignored three-site cumulants.

Cumulants involving four or more sites can be similarly computed. The concept of "nontrivial partitions" is generalized in the obvious way. For the galaxy problem any distinct four neighbors of a site α will contribute (for the four-site cumulant) and there are $\binom{6}{4} = 15$ such terms. The effect of such a term will go as p^8 (corresponding to p^6 for three-site cumulants) and may be expected to be of even less importance.

NOTE ADDED IN PROOF

Monte Carlo simulations have been used to measure γ, the mean cluster size exponent (cf. Blease[10]). We find in $1+1$ dimensions $\gamma = 2.11 \pm 0.15$ and in $2+1$ dimensions $\gamma = 1.50 \pm 0.10$.

REFERENCES

1. H. Gerola and P. E. Seiden, *Astrophys. J.* **223**:129 (1978).
2. P. E. Seiden and H. Gerola, *Astrophys. J.* **233**:56 (1979).
3. H. Gerola, P. E. Seiden, and L. S. Schulman, *Astrophys. J.* **242**:517 (1980).
4. P. E. Seiden, L. S. Schulman, and H. Gerola, *Astrophys. J.* **232**:702 (1979).
5. C. C. Lin and Y. Y. Lau, *Stud. Appl. Math.* **60**:97 (1979).
6. M. Kimura, in *Mathematical Topics in Population Genetics*, K. I. Kojima, ed. (Springer, New York, 1970).
7. C. M. Newman and L. S. Schulman, *J. Stat. Phys.* **23**:131 (1980).

8. L. S. Schulman and P. E. Seiden, *J. Stat. Phys.* **19**:293 (1978); also IBM Research Report, Statistical mechanics of a dynamical system based on Conway's game of life, 1977, containing the above paper plus appendixes on cumulants and other topics.
9. J. G. Mauldon, *Proc. Fourth Berkeley Sympo.* **1**:337 (1961).
10. J. Blease, *J. Phys. C.* **10**:917 (1977).
11. C. M. Newman and L. S. Schulman, in preparation.
12. V. K. S. Shante and S. Kirkpatrick, *Adv. Phys.* **20**:325 (1971).